Materials Science & Engineering A 624 (2015) 79–89

Contents lists available at ScienceDirect

Materials Science & Engineering A

journal homepage: www.elsevier.com/locate/msea

Room-temperature creep and stress relaxation in commercial purity titanium–Influence of the oxygen and hydrogen contents on incubation phenomena and aging-induced rejuvenation of the creep potential

B. Barkia [a,b], V. Doquet [a,*], J.P. Couzinié [b], I. Guillot [b]

[a] Laboratoire de Mécanique des Solides, CNRS UMR7649, Ecole Polytechnique, Palaiseau, France
[b] Institut de Chimie et des Matériaux de Paris Est, CNRS / UPEC UMR 7182, Thiais, France

ARTICLE INFO

Article history:
Received 25 September 2014
Received in revised form
18 November 2014
Accepted 21 November 2014
Available online 1 December 2014

Keywords:
Titanium
Creep
Relaxation
Strain aging
Oxygen
Hydrogen

ABSTRACT

Creep and stress relaxation tests were run at room-temperature along the rolling and transverse directions in three batches of titanium with different solute oxygen and hydrogen contents. Oxygen-induced dynamic strain aging was shown to hinder creep at low stress level and solute hydrogen to enhance it and to promote a dramatic aging-induced rejuvenation of the creep potential. Primary creep could be described by a single power law equation in which both the anisotropy and the influence of the oxygen content were taken into account. Secondary creep rates varied exponentially with the applied stress, in the same way along rolling and transverse directions, but with a stress dependency which increased with the oxygen content. Creep of commercial purity titanium was controlled mainly by screw dislocations with a ⟨1–210⟩ Burgers vector gliding on prismatic and pyramidal planes, while for a Ti batch with a lower oxygen content and larger grain size, mechanical twinning also contributed to the creep strain. 33–40% of the flow stress was relaxed within 20 h, according to logarithmic kinetics, which did not depend on the loading direction or oxygen content.

1. Introduction

In 1949, Adenstedt [1] first reported room-temperature primary creep in commercial purity (CP) titanium at stresses as low as 60% of the yield stress, followed by secondary creep and then tertiary creep and terminal failure above 90% of the yield stress. Primary creep may induce strains at room temperature substantial enough to deserve being accounted for in structural design.

There has been a renewed interest in this subject during the last two decades, due to several industrial applications for which low-temperature creep of commercially-pure titanium may be an issue: such is the case of the drip shield for nuclear waste storage in the USA [2,3] or the container itself in Canada [4], bolts, nuts and fuel tanks for satellites [5,6], expansion joints in heat exchangers that become loose and cause leakage [7], creep at crack tips in welded parts in submarines causing subcritical crack growth due to residual stresses [8], or even potential creep problems in biomedical applications of ultrafine grained CP titanium.

Kiessel and Sinnott [10] found that the creep resistance of titanium does not decrease regularly with increasing temperature, but exhibits a maximum at 200 °C attributed to strain aging. This peak in creep resistance was confirmed by Luster et al. [11]. Scholl and Knorr [12] noticed the unusual shape of creep curves in CP titanium between 20 °C and 300 °C and attributed it to the interactions between gliding dislocations and solute impurities. Nonetheless, Severac et al. [13,14] reported an abnormal evolution of the creep resistance with the temperature in the range 150–400 °C, even in high-purity titanium (25 ppm O, 25 ppm Fe). According to Zeyfang et al. [15], the rate-controlling process during low temperature creep of titanium (−200 to 77 °C) is the thermally-activated overcoming of solute obstacles. This is consistent with the conclusions drawn by Stetina [16] that creep of titanium is controlled by the overcoming of interstitials by dislocations gliding in prism planes up to a critical temperature. Above this temperature it would become nearly athermal and mainly controlled by the grain size. The transition temperature – close to 150 °C – would decrease with the interstitial content.

Matsunaga et al. [5] reported, for titanium and other H.C.P. metals, an inverse dependence of the room-temperature steady-state creep rate on the grain size, as well as a very low activation energy for creep ($Q \approx 20$ kJ/mol) they attributed to grain-boundary sliding.

* Corresponding author. Tel.: +33 16 933 5765; fax: +33 16 933 5706.
E-mail address: doquet@lms.polytechnique.fr (V. Doquet).

http://dx.doi.org/10.1016/j.msea.2014.11.073
0921-5093/

According to their AFM measurements of out-of-plane slip offsets, grain boundary sliding might significantly contribute to the creep strain, even at room temperature. By contrast, Oberson et al. [17,18] observed an increase in low-temperature creep rate in Ti–1.6 wt% V and Ti–0.4 wt% Mn with the grain size. The effect was attributed to a slow, oxygen diffusion-controlled growth of twins, which form more easily in large grains. According to Matsunaga et al. [6] mechanical twinning would, on the contrary, hinder room-temperature creep in CP titanium. According to Severac et al. [13] the main deformation mode during creep of grade 2 titanium is dislocation glide, with minor contributions of mechanical twinning and kink bands formation, while grain boundary sliding would occur only at high temperatures. There is an obvious lack of consensus about the mechanisms that control room-temperature creep in C.P. titanium. Furthermore, unlike Ti alloys for which thorough TEM observations of creep-induced dislocation structures were made [19,20], only limited work of that type [6] is available for C.P. titanium.

The transition between primary creep leading to creep exhaustion and primary creep followed by secondary creep occurs within a very narrow range of stress. Paties [9] found that in Grade 4 titanium, the transition stress depends on the strain rate during the loading stage: it was 0.7 to $0.8\sigma_{0,2}$ for 10^{-3} s^{-1} and $0.9\sigma_{0,2}$ for 10^{-5} s^{-1}.

Data on secondary creep rates at room temperature is scarce in the literature and not quite consistent. Matsunaga et al. [5] report stress exponents of 3, 5.5 and 6, respectively for titanium batches containing 400, 600 and 900 ppm oxygen tested between 0.6 and $0.9\sigma_{0.2}$. By contrast, the minimum creep rate versus stress plot reported by Sato et al. [21] as well as by Tanaka et al. [22] for grade 2 titanium with 1500–2000 ppm oxygen are bi-linear, with an exponent of 4–5 below $0.8\sigma_{0.2}$ and a sharp increase in slope, or power law breakdown (PLB) above. In Grade 4 titanium, Paties [9] found a very high stress exponent of 29, or in other words, PLB.

No data seem to be available as concerns the influence of hydrogen on room-temperature creep in C.P. titanium, but it is worth mentioning those available on creep in Ti alloys. Gao and Dexter [23] observed that at a given creep stress, increasing the H content of Ti6Al4V from 80 to 720 ppm increased the 100 h primary creep strain linearly, with an increase in slope when the applied stress rose. TEM observations did not reveal any hydrides or any qualitative modification of dislocations structures. It was thus concluded that solute hydrogen does not change the primary creep mechanisms but just enhances screw dislocations mobility. Hardie and Ouyang [24] as well as Mignot et al. [25] also reported an acceleration of room-temperature creep in hydrogen-charged Ti6Al4V and Ti6246, respectively. Gerland et al. [26] observed contrasted effects of solute hydrogen on room-temperature creep of Ti6242, depending on the stress level and thus on the creep rate. At $0.9\sigma_{0.2}$, an acceleration of creep was observed when the solute H content increased, while the reverse effect was found at $\sigma_{0.2}$.

Zirconium and titanium share many properties. In that respect, it is pertinent to mention that, according to Rupa [27], solute hydrogen accelerates creep in recrystallized Zircaloy, especially in the temperature range where oxygen-induced dynamic strain aging is present (between 300 and 400 °C), while hydrides tend to slow creep down.

Note that all existing studies on C.P. Titanium focused on creep along the rolling direction – in which case prismatic glide predominates – and not in other directions that might promote other deformation mechanisms, such as pyramidal ⟨a⟩ and ⟨c+a⟩ slip, and mechanical twinning. The creep anisotropy of titanium is thus not documented.

The work presented in this paper constitutes a part of a multi-scale investigation of the viscoplastic behaviour and sustained-load cracking of titanium at room-temperature, under the combined influence of solute oxygen and hydrogen. The present paper deals with the influence of oxygen and hydrogen contents on room-temperature creep and stress relaxation. It also provides some elements about the creep mechanisms, based on TEM observations.

2. Materials and experimental procedures

Cylindrical specimens with a 8 mm diameter and a 16 mm gage length were cut along the rolling or transverse directions (RD, TD) from a 20 mm-thick plate of grade 2 titanium (denoted below as T40) and a 26 mm-thick plate of grade 4 titanium (denoted as T60). A few additional specimens were cut in the transverse plane of a higher purity forged billet, 110 mm in diameter. The latter material will be denoted as Ti0. Table 1 indicates the chemical compositions of the materials. The oxygen and hydrogen contents were measured by Bureau Veritas by inert gas fusion analysis, using a LECO RH402 apparatus that performs conductivity measurements for hydrogen analysis and a LECO TC500 apparatus that performs infrared absorption measurements, for oxygen analysis. Most specimens were annealed during 12 h at 500 °C under secondary vacuum. These specimens will be designated by “as-received”.

Fig. 1 shows the pole figures obtained by EBSD mappings over 1×1 mm^2 areas. Classical textures of rolled plates are observed in T40 as well as in T60, with the ⟨c⟩ axes normal to the rolling direction, tilted towards the TD by 30–90° and {10–10} directions

Table 1
Chemical compositions of the materials.

Material	O (wt. ppm)	C (wt. ppm)	N (wt. Ppm)	$O_{eq.}$ (at%)	H (wt. Ppm)	H (at %)	O_{eq}/H (at. Ratio)	Fe (wt%)
Ti0	450 ± 30	< 80	< 30	0.135	5 ± 2	0.023	6.0	0.0007
T40	1600 ± 50	40	30	0.510	7 ± 2	0.028	15.9	0.0340
T60	3200 ± 100	70	60	1.020	15 ± 3	0.075	13.6	0.1800

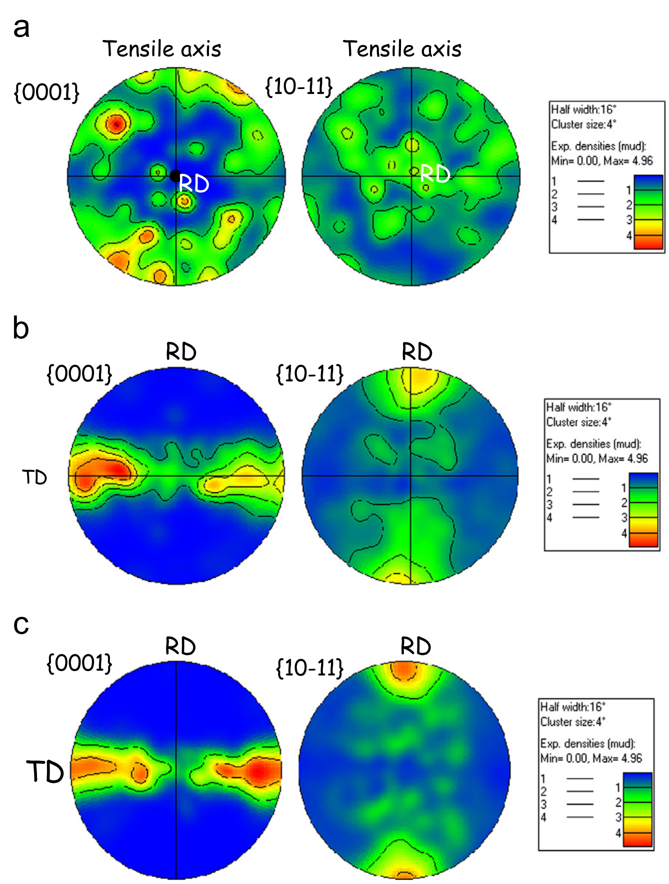

Fig. 1. Pole figures for (a) Ti0, (b) T40 and (c) T60.